HHS Public Access

Author manuscript

Acta Biomater. Author manuscript; available in PMC 2021 August 01.

Published in final edited form as:

Acta Biomater. 2020 August ; 112: 250–261. doi:10.1016/j.actbio.2020.06.001.

Pendant-bearing glucose-neopentyl glycol (P-GNG) amphiphiles for membrane protein manipulation: Importance of detergent pendant chain for protein stabilization

Hyoung Eun Bae[a], **Cristina Cecchetti**[b], **Yang Du**[c], **Satoshi Katsube**[d], **Jonas S. Mortensen**[e], **Weijiao Huang**[c], **Shahid Rehan**[f,g], **Ho Jin Lee**[a], **Claus J. Loland**[e], **Lan Guan**[d], **Brian K. Kobilka**[c], **Bernadette Byrne**[b], **Pil Seok Chae**[a]

[a]Department of Bionanotechnology, Hanyang University, Ansan, 15588 (Korea) [b]Department of Life Sciences, Imperial College London, London, SW7 2AZ (UK) [c]Department of Molecular and Cellular Physiology, Stanford University, CA 94305 (USA) [d]Department of Cell Physiology and Molecular Biophysics, Center for Membrane Protein Research, School of Medicine, Texas Tech University Health Sciences Center, Lubbock, TX 79430 (USA) [e]Department of Neuroscience, University of Copenhagen, Copenhagen, DK-2200 (Denmark) [f]Institute of Biotechnology, University of Helsinki, Helsinki (Finland) [g]HiLIFE, University of Helsinki, Helsinki (Finland)

Abstract

Glucoside detergents are successfully used for membrane protein crystallization mainly because of their ability to form small protein-detergent complexes. In a previous study, we introduced glucose neopentyl glycol (GNG) amphiphiles with a branched diglucoside structure that has facilitated high resolution crystallographic structure determination of several membrane proteins. Like other glucoside detergents, however, these GNGs were less successful than DDM in stabilizing membrane proteins, limiting their wide use in protein structural study. As a strategy to improve GNG efficacy for protein stabilization, we introduced two different alkyl chains (i.e., main and pendant chains) into the GNG scaffold while maintaining the branched diglucoside head group. Of these pendant-bearing GNGs (P-GNGs), three detergents (GNG-2,14, GNG-3,13 and GNG-3,14) were not only notably better than both DDM (a gold standard detergent) and the previously described GNGs at stabilizing all six membrane proteins tested here, but were also as efficient as DDM at membrane protein extraction. The results suggest that the C14 main chain of the P-GNGs is highly compatible with the hydrophobic widths of membrane proteins, while the C2/C3 pendant chain is effective at strengthening detergent hydrophobic interactions. Based on the marked effect on protein stability and solubility, these glucoside detergents hold significant potential for membrane protein structural study. Furthermore, the independent roles of the detergent two alkyl chains first introduced in this study have shed light on new amphiphile design for membrane protein study.

pchae@hanyang.ac.kr.

Author disclosure statement

The authors have no conflicts of interest to declare.

Supplementary data

Supplementary data to this article can be found online at https://doi.org/10.1016/j.actbio.2020.06.001.

Keywords

amphiphiles; membrane proteins; protein stabilization; amphiphile design; protein structure

1. Introduction

Membrane proteins are essential components of cell membranes and play vital roles in a variety of cellular functions such as material transport, signal transduction and cell-to-cell recognition. Membrane proteins coded in the human genome account for ~25% of the total proteome. Malfunctions of these bio-macromolecules are implicated in various diseases including cystic fibrosis, atherosclerosis, Parkinson's and Alzheimer's diseases [1,2]. The importance of membrane proteins in human health can be illustrated by the fact that more than 50% of marketed pharmaceuticals target membrane-inserted proteins [3]. Despite tremendous efforts, however, obtaining high resolution membrane protein structures is still extremely challenging due in part to their marked tendency to aggregate or denature in aqueous solution [4,5]. Only 2~3% of proteins with known structures correspond to membrane proteins [6-8]. The slow progress in membrane protein structural study is mainly due to the presence of the large hydrophobic surfaces that need to be effectively shielded by a membrane-like system.

Micelles formed by conventional detergents such as *n*-octyl-β-D-glucoside (OG), *n*-decyl-β-D-maltoside (DM) and *n*-dodecyl-β-D-maltoside (DDM) are widely used for membrane protein study [9,10]. Due to their amphiphilic properties, detergent micelles have the ability to associate with the hydrophobic surfaces of membrane proteins, making the resulting protein-detergent complexes (PDCs) water-soluble [11,12]. Although conventional detergents are generally good at protein extraction from the membranes, many membrane proteins, particularly from eukaryotic sources, are unstable in detergent-based solution. Developing new detergents that combine high protein extraction efficiency with long term protein stability, remains extremely challenging [13]. For example, lauryldimethylamine-*N*-oxide (LDAO), a zwitterionic detergent, is efficient for protein extraction, but it is estimated that only 20% of all membrane proteins are stable in this detergent [14]. In contrast, DDM, a non-ionic maltoside detergent, is significantly better than LDAO at protein stability in most cases, but tends to be less efficient than the zwitterionic detergent when it comes to protein extraction.

Over the last two decades, several amphipathic systems have been developed with a view to overcoming the limitation of conventional detergents in membrane protein stabilization. Representative examples include lipidic systems surrounded by detergent/protein [bicelles and nanodiscs (NDs)][15], peptide-based detergents [lipopeptide detergents (LPDs) and β-peptide (BPs)][14,16] and amphiphilic polymers [amphipols (APols) and styrene-maleic acid (SMA) copolymer][17-19]. These new systems effectively stabilize membrane proteins, but most are not efficient at extracting from the membranes and tend to be suboptimal for membrane protein crystallization. As alternatives to conventional detergents, small amphipathic molecules have also been devised for membrane protein manipulation. These small amphiphiles typically have multiple alkyl chains as the hydrophobic group, as

exemplified by neopentyl glycol-based amphiphiles [glucose neopentyl glycols (GNG), maltose neopentyl glycols (MNGs) and neopentyl glycol-derived triglucosides (NDTs)] [20-22], mannitol-based amphiphiles (MNAs)[23], resorcinarene-based glucoside amphiphiles (RGAs)[24], penta-saccharide-bearing amphiphiles (PSEs)[25], dendronic hydrophobic group-bearing trimaltosides (DTMs)[26], and stereoisomeric detergents [(butane-1,2,3,4-tetraol-based maltosides (BTMs) and norbornane-based maltosides (NBMs)][27,28]. These amphipathic molecules proved to be effective both at protein stabilization and membrane protein extraction. Of the newly developed amphiphiles, MNG-3 (i.e., LMNG) is notable as this agent has facilitated high resolution structure determinations of more than 30 membrane proteins including several G protein-coupled receptors (GPCRs) [29-39]. This MNG has been most successfully used in combination with lipidic cubic phase crystallization approaches (LCP) (i.e. *in meso* method) [40]. Very recently, oligoglycerol-based detergents (OGDs) with particular promise for native mass analysis of membrane proteins have been developed [41].

Although less effective than DDM at protein stabilization, GNG-3 (i.e., OGNG) is compatible with *in-surfo* protein crystallization as demonstrated by high resolution crystal structures of several membrane proteins [42-46]. This result indicates that OGNG has characteristics favorable for *in surfo* protein crystallization, likely originating from the possession of the smaller glucoside rather than the maltoside headgroup. Glucoside detergents (e.g., OG and OGNG) tend to form small PDCs, improving crystal packing *via* enhanced hydrophilic protein-protein interactions [47,48]. However, they are typically less effective at stabilizing membrane proteins than DDM. Thus, it is important to develop new glucoside detergents that provide enhanced protein stability compared to the conventional detergent, without any associated loss in protein extraction ability. In this study, we present a class of detergents obtained by introducing hydrophobic variations into the previously developed GNG scaffold [20]. Along with a long main chain, these GNG variants, designated pendant-bearing GNGs (P-GNGs), have a short pendant chain at the interface between the hydrophobic and hydrophilic groups. Results show that some of the P-GNGs were not only efficient at extracting membrane proteins, but also were notably effective at stabilizing all the membrane proteins tested here, including two G-protein-coupled receptor (GPCRs), compared to the gold standard detergent (DDM). In addition, the role of the pendant chain introduced here would shed light on future design of new detergents useful for membrane protein research

2. Materials and Methods

2.1. AtBOR1 stability assay

2.1.1. CPM assay—The BOR1 from *Arabidopsis thaliana* was expressed as a fusion protein with a C-terminal TEV-cleavable GFP-8His tag in *Saccharomyces cerevisiae* FGY217 cells [49]. The cells were grown in -URA media supplemented with 0.1% glucose. Protein expression was induced with addition of 2% galactose followed by an incubation for 22 hours at 30 °C as previously described [49]. The cells were harvested and used to prepare membranes as previously described [50]. Membranes containing AtBOR1 were resuspended in PBS (pH 7.4), 100 mM NaCl, 10% glycerol and solubilized in 1% DDM for 1 hour with a

mild agitation followed by ultracentrifugation at 200,000 *g* for 45 min. The supernatant was adjusted to 10 mM imidazole and applied to two 5 mL Ni^{2+}-NTA columns pre-equilibrated with Buffer A (PBS (pH 7.4), 100 mM NaCl, 10% glycerol, 0.03% DDM) supplemented with 10 mM imidazole. The column was washed with 5 CV of Buffer A supplemented with 30 mM imidazole, then 5 CV of Buffer A supplemented with 50 mM imidazole, followed by elution in Buffer A supplemented with 500 mM imidazole. The fractions containing AtBOR1- GFP were diluted (1:10) in Buffer B (20 mM Tris (pH 7.5), 150 mM NaCl, 0.03% DDM) supplemented with 10% glycerol and incubated overnight with an equimolar concentration of His-tagged TEV protease to cleave the GFP-His tag. The sample was applied to a 5 mL Ni^{2+}-NTA column pre-equilibrated with Buffer B supplemented with 20 mM imidazole to separate AtBOR1 from the GFP-His tag and the TEV. The flow-through containing AtBOR1 was concentrated to 0.5 mL using centrifugal concentrators. The protein underwent a final gel filtration purification step using a Superdex 200 10/300 column (GE Healthcare) pre-equilibrated with Buffer B containing 0.03% DDM. AtBOR1 was concentrated to 10 mg/mL using centrifugal concentrators. *N*-[4-(7-diethylamino-4-methyl-3-coumarinyl)phenyl] maleimide (CPM) dye (Invitrogen) at 4 mg/mL stored in DMSO (Sigma), was diluted (1:100) in assay buffer (20 mM Tris (pH 7.5), 150 mM NaCl) supplemented with 0.03% DDM [51]. A Nunc 96-well clear bottom plate was loaded with 150 μL of the assay buffer (20 mM Tris-HCl (pH 7.5), 150 mM NaCl) supplemented with either CMC + 0.04 wt% or CMC + 0.20 wt% of the P-GNGs, OGNG or DDM. 1 μL of AtBOR1 (~10 mg/mL) in 0.03% DDM was added to each well before adding 3 μL diluted CPM dye, resulting in 150-fold dilution of the DDM-purified AtBOR1. A clear plate cover was added and the fluorescence of each well was monitored every 5 minutes at 40 °C for 120 minutes using a SpectraMax M2 (Molecular Devices) with an excitation wavelength of 387 nm and an emission wavelength of 463 nm.

2.1.2. Fluorescence size exclusion chromatography (FSEC)—The membranes containing BOR1-GFP fusion proteins were diluted to a final total protein concentration of 2.8 mg/mL in PBS (pH 7.4) supplemented with either 1% DDM, OGNG, or one of the individual P-GNGs (GNG-3,13 GNG-2,14 and GNG-3,14). The samples were incubated with gentle rocking for 1 hour at 25 °C and then the insoluble material was removed by centrifugation at 14 000 g for 1 hour at 4 °C. The supernatants containing the solubilized protein samples were heated at 46 °C for 10 minutes. After a further centrifugation to remove any large aggregates, a 200 μL aliquot of the supernatant was injected onto a Superose 6 10/300 column (GE Healthcare) equilibrated with 20 mM Tris (pH 7.5), 150 mM NaCl and 0.03% DDM. The GFP fluorescence of each fraction was read using an excitation wavelength of 470 nm and an emission wavelength of 512 nm.

2.1.3. Molecular weight determination of AtBOR1 purified in DDM—100 μL purified AtBOR1 at 0.4 mg/mL was injected onto a Superdex-200 10/300 gel filtration column (GE Healthcare) equilibrated in Buffer B. The elution was assessed with a miniDAWN TREOS and an Optilab rEX detection system (Wyatt Technology) and the data analyzed using ASTRA 6.1.1.17 (Wyatt Technology). To determine the molecular weight of AtBOR1, the molecular weight of the DDM micelle (144 ± 2 kDa) was subtracted from the measured molecular weight of the protein-detergent complex.

2.2. LeuT stability assay

Purification of the wild type of the leucine transporter (LeuT) from *Aquifex aeolicus* was performed according to the protocol described previously [52]. The transporter (LeuT) was expressed in *E. coli* C41 (DE3) cells transformed with pET16b encoding the 8xHis-tagged transporter. The isolated protein was solubilized in 1.0 % DDM and bound to Ni^{2+}-NTA resin (Life Technologies, Denmark). The resin-bound transporter protein was eluted with elution buffer containing 20 mM Tris-HCl (pH 8.0), 1 mM NaCl, 199 mM KCl, 0.05% DDM and 300 mM imidazole. Subsequently, 100 μL of purified protein stock (approximately 1.5 mg/mL) was added to 900 μL identical buffer without DDM and imidazole, but supplemented with the respective P-GNG, OGNG and DDM (control) (e.g. 10-fold dilution). The protein samples were equilibrated at room temperature for 16 hours before first measurement. The final detergent concentrations were CMCs + 0.04 wt% or CMCs + 0.20 wt%. For detergent comparison, LMNG was included in the detergent evaluation at CMCs + 0.20 wt%. The protein samples were stored for 11 days at room temperature and protein activity was determined by measuring [^{3}H]-leucine ([^{3}H]-Leu) binding using the scintillation proximity assay (SPA) [53]. SPA was performed at the designated detergent concentrations with 5 μL of the respective protein samples, 20 nM [^{3}H]-Leu and 1.25 mg/mL copper chelate (His - Tag) YSi beads (both from Perkin Elmer, Denmark) in buffer containing 450 mM NaCl. [^{3}H]-Leu binding was determined using a MicroBeta liquid scintillation counter (Perkin Elmer).

2.3. β_2AR stability assay

β_2AR was purified in a buffer (20 mM HEPES pH 7.5, 100 mM NaCl, 0.1% DDM) at a concentration of 1.0 μM as described previously [54]. The DDM-purified β_2AR was diluted 150-fold using buffer solutions containing individual detergents (P-GNGs, OGNG and DDM) to give final detergent concentrations of CMCs+0.2 wt%. The receptor in each detergent was stored for 5 days at room temperature and its ligand binding capacity was measured at regular intervals by incubating the receptor with 10 nM of radioactive [^{3}H]-DHA for 30 min at room temperature. The mixture was loaded onto a G-50 column and the flow-through was collected in binding buffer (20 mM HEPES pH 7.5, 100 mM NaCl, supplemented with 0.5 mg/mL BSA), followed by addition of 15 mL scintillation fluid. Receptor-bound [^{3}H]-DHA was measured with a scintillation counter (Beckman).

2.4. MelB stability assay

2.4.1. MelB solubilization and thermal stability—

E. coli DW2 strain (Δ*melB* and Δ*lacZY*) harboring pK95ΔAHB/WT $MelB_{St}$/CH10 plasmid were used to produce the protein [55,56]. The plasmid contains the gene encoding the melibiose permease of *Salmonella typhimurium* ($MelB_{St}$) with a 10-His tag at the C-terminus. Cell growth and membrane preparation were carried out as described [56]. The membrane samples containing $MelB_{St}$ (at a final concentration of 10 mg/mL) were treated with individual detergents (DDM, OGNG, or a P-GNG) at 1.5 wt% in a buffer containing 20 mM sodium phosphate, pH 7.5, 200 mM NaCl, 10% glycerol and 20 mM melibiose. Protein extractions were carried out at 0 °C for 90 min and further treated at 0 °C or three other different temperatures (45, 55, and 65 °C) for another 90 min [56,57]. Insoluble fractions were

removed by ultracentrifugation at 95,000 rpm in a Beckman OptimaTM MAX ultracentrifuge using a TLA-100 rotor for 45 minutes at 4 °C. Detergent-extracted $MelB_{St}$ was analyzed by SDS-15% PAGE after ultracentrifugation. An untreated membrane sample, designated Memb, was used as a reference. The transporter was visualized by immunoblotting with a HisProbe-HRP antibody (Thermo Scientific).

2.4.2. Trp→D^{2}G FRET assay—Bacterial right-side-out (RSO) membrane vesicles were prepared via osmotic lysis from *E. coli* DW2 cells expressing $MelB_{St}$ or $MelB_{Ec}$ in a buffer containing 100 mM KPi (pH 7.5) and 100 mM NaCl [56,57]. A transporter ($MelB_{St}$ or $MelB_{Ec}$ at 1 mg/ml in 1.0 wt% of DDM or GNG-3,14) at 23 °C was subjected to ultracentrifugation using TLA 120.2 rotor at > 300,000 g for 45 minutes at 4 °C. The supernatants were used for Trp→D^{2}G (2'-(*N*-Dansyl)aminoalkyl-1-thio-β-D-galactopyranoside) FRET experiments using an Amico-Bowman Series 2 (AB2) Spectrofluorometer. D^{2}G FRET signals were collected at 490 and 465 nm for $MelB_{St}$ and $MelB_{Ec}$, respectively. On a time trace, 10 μM D^{2}G and excess melibiose or equal volume of water were added at 1-min and 2-min time points, respectively.

2.5. MOR thermostability assay (CPM assay)

CPM dye in DMSO (3 mg/mL stock) was diluted 40x in buffer containing 20 mM HEPES pH 7.5 and 150 mM NaCl [51]. The mouse μ-opioid receptor (MOR) was purified in a buffer containing 20 mM HEPES 7.5, 100 mM NaCl and DDM (0.05%)/CHS (0.005%) at a stock concentration of 20 μM, which was diluted to 4 μM (DDM 0.01%) in 250 μL of 1.0 % solutions of P-GNGs (GNG-2,14, GNG-3,13, and GNG-3,14), LMNG, and DDM. After one-hour incubation at room temperature, the receptor solution was further diluted two-fold in 20 mM HEPES (pH 7.5), 150 mM NaCl to reach the final detergent concentration of 0.5 wt%. Receptor stability in the different detergents was measured by adding 5 μL of the diluted CPM dye and then recording the fluorescence spectra (excitation 387 nm) from 20 to 65 °C at every 5 °C with a two-minute incubation at each temperature. The melting temperature (T_m) of the detergent-solubilized receptor was computed by plotting the reading at 470 nm and fitting a non-linear regression curve using GraphPad Prism.

2.6. hENT1 stability assay

2.6.1. Expression of hENT1, isolation of membranes and detergent solubilization—Insect cell expression of human equilibrative nucleoside transporter 1 (hENT1; NCBI gene ID: 2030) was carried out as described previously [58]. After expression cells were collected by centrifugation at 1000 *g* for 5 minutes and disrupted in lysis buffer (50 mM HEPES, pH 8.0, 500 mM NaCl, 5 mM EDTA, and 1 mM PMSF) by dounce homogenization. Membranes were prepared as described previously [58]. Briefly, unbroken cells were separated by centrifugation at 1000 *g* for 10 minutes and membranes were isolated by ultracentrifugation at 235,000 *g* for 1 hour. Isolated membranes were re-suspended in ice-cold buffer (50 mM HEPES, pH 8.0, 500 mM NaCl) and washed 3 to 4-times. Finally, membranes were re-suspended in storage buffer (50 mM HEPES, pH 8.0, 500 mM NaCl and 20% glycerol) and stored at − 70 °C until further analysis. hENT1-expressing Sf9 membranes were diluted to a final protein concentration of 3 mg/mL in buffer containing 50 mM HEPES, pH 8.0, 500 mM NaCl, and 10% glycerol, and then solubilized

with 1% of each detergent (GNG-2,14, GNG-3,14, or DDM) at 4 °C for 1 hour. Insoluble protein was separated by ultracentrifugation at 235,000 *g* for 30 minutes, and supernatant containing detergent-solubilized hENT1 was collected for further analysis.

2.6.2. Analysis of hENT1 stability—Stability of hENT1 in the individual detergents was monitored using a radioligand-binding assay as described previously [58,59]. Briefly, 100 μL of solubilized hENT1 sample from each detergent (GNG-2,14, GNG-3,14, or DDM) was transferred into thin wall PCR tubes and incubated at 4, 40, 45, and 50°C for 30 minutes followed by ultracentrifugation at 235,000 *g* for 30 minutes. Supernatants were collected in fresh tubes and used for radioligand binding assay as follows. Detergent-solubilized hENT1 samples were incubated with 5 nM [^{3}H]-nitrobenzylmercaptopurine ribonucleoside (NBMPR) for 30 min at 22 °C. In order to assess non-specific ligand binding, identical reactions were prepared in the presence or absence of 10 μM dipyridamole. Reaction was loaded on 96-well sephadex G-50 gel filtration plate and unbound ligand was removed by centrifugation at 2000 rpm for 5 minutes. Protein-ligand complex was collected as void volume and filtrate was transferred to fresh 96 well plate pre-filled with OptiPhase scintillation liquid. Radioactivity was measured using a MicroBeta TriLux scintillation counter (Millipore). The amount of [^{3}H]-NBMPR specifically bound to hENT1 was calculated as the difference between the amount of [^{3}H]-NBMPR that bound in the presence and absence of 10 μM dipyridamole. Data was analyzed using Graphpad prism software.

2.7. Statistical Analysis

The experiments were repeated at least two times as presented in each caption. All data were expressed in terms of mean ± standard deviation (SD) or standard error of the mean (SEM). Statistical analysis was performed with GraphPad 6.0 software (GraphPad Software Inc., San Diego, CA, USA).

3. Results

3.1. Detergent design and physical characterizations

GNG variants introduced in this study share a branched diglucoside headgroup with the previously developed GNGs (Scheme 1). However, the previous GNGs have two identical alkyl chains in the lipophilic region, while the new variants have two different alkyl chains (long main and short pendant chains) in the same region. The main chain varied from *n*-undecyl (C11) to *n*-tetradecyl (C14) group. The short pendant chain varying from methyl (C1) to *n*-propyl (C3) was introduced so that it is positioned at the interface between the detergent hydrophobic and hydrophilic groups. These variations in the main and pendant chain lengths, incorporated in the detergent designation, are necessary to find an optimal hydrophile-lipophile balance (HLB), a key detergent property for membrane protein stability [60,61]. Similar pendant-bearing detergents have been reported, but these detergents have a maltoside headgroup rather than a branched diglucoside (Scheme 1) [62]. Furthermore, these maltoside detergents were not better than the original maltoside (DDM) for membrane protein stability. Due to the presence of the different headgroups (branched diglucoside *vs* maltoside), the P-GNGs would form compact and stable micelles compared to the previous DDM analogues, thereby being more effective for membrane protein stability.

Each P-GNG was prepared according to a reported protocol using diethyl malonate as the starting material [63]. A long alkyl chain was first attached into the α-carbon of the malonate, followed by attachment of the second alkyl group (i.e., pendant chain) into the same position using methyl, ethyl, or propyl halide. The resulting tetraester compound was reduced to the dialkylated tetra-ol derivative, which was used as a substrate of β-selective glycosylation. The β-stereochemistry of the glycosidic bonds was confirmed by individual ^{1}H NMR spectra of the P-GNGs isolated after a global deprotection (Fig. S1). All P-GNGs showed a doublet peak at 4.32 ppm with a vicinal coupling constant of J = 8.0 Hz in their spectra. These chemical shift (δ) and coupling constant (J) are strong indications of β-glycosidic bond formation. The differences in the two alkyl chain lengths (main and pendant chains) were recognizable in the ^{1}H NMR spectra of the ethyl pendant-bearing GNGs (GNG-2,11, GNG-2,12, GNG-2,13 and GNG-2,14). The peak of the protons attached to the long alkyl tip appears as a triplet at 0.90 ppm, while the protons of the short alkyl tip give rise to a triplet peak at 0.83 ppm (Fig. S1). The differences in chemical shift between the protons of the long and short alkyl tips were negligible for the case of the other P-GNGs.

The P-GNGs have a range of total carbon number in the alkyl chain from 12 (GNG-1,11) to 17 (GNG-3,14) and all these agents were highly water-soluble up to 10 wt%. The good water-solubility of these P-GNGs, a prerequisite of detergent utility in membrane protein study, are interesting as a previous GNG with two heptyl chains (i.e., GNG-7,7) showed less than 1.0 wt% water-solubility (Scheme 1a). This enhanced water-solubility is likely due to effective hydrophobic interactions between the detergent alkyl chains in micelles formed by the P-GNGs. Detergent CMCs were estimated by using a hydrophobic fluorescent dye, diphenylhexatriene (DPH) (Table 1) [64]. Two GNGs, GNG-1,11 and GNG-6,6 (i.e., OGNG), have the same total carbon number (C12) in their alkyl chains, thus being isomeric to each other. However, the CMC of GNG-1,11 was six-fold lower than the CMC of OGNG (170 vs 1000 μM), supporting the strong hydrophobic interactions of the P-GNGs relative to OGNG in the micellar environment. As expected, the CMCs of the P-GNGs reduced with increasing alkyl chain length. For instance, the CMC values of the methyl pendant-bearing GNGs decreased from 190 to 100 to 38 to 26 μM with increasing main chain length from C11 to C12 to C13 to C14. With the main chain length kept at C11, the CMCs of the P-GNGs gradually reduced from 190 to 150 to 100 μM with pendant chain length increasing from C1 to C2 to C3.

Micelle sizes formed by the P-GNGs were measured by dynamic light scattering (DLS) and represented as hydrodynamic radii (R_h) (Table 1). Overall, all P-GNGs form smaller micelles than OGNG (4.46 nm) and DDM (3.47 nm), again supporting effective hydrophobic interactions in the micelle interiors. Detergent micelles gradually enlarged with increasing main chain length as exemplified with R_h values of 2.81 (GNG-1,11), 2.93 (GNG-1,12), 3.08 (GNG-1,13) and 3.25 nm (GNG-1,14). This variation in micelle size could be explained by the relative volume of the detergent head and tail groups [65]. In contrast, micelle size was unaffected by variation in the pendant chain length. For example, all P-GNGs with the C11 and C14 alkyl chains, independent of their pendant chain lengths, form micelles with a R_h of 2.76-2.82 and 3.20-3.26 nm, respectively. This result indicates that micelle sizes formed by the P-GNGs are primarily determined by the main chain length, which in turn suggests that the variation in the pendant chain length (C1 to C3) has little

effect on the molecular geometry of the P-GNGs. Detergent micelles were further analyzed in terms of size distribution of their populations. When micelle size distributions were represented by number- and volume-weighted DLS profiles, all P-GNG micelles showed a single set of populations with small sizes (Fig. 1, S2, & S3). Large micelle populations with a size range of 100~1000 nm detected in intensity-weighted profiles are due to the ultra-high sensitivity of light scattering intensity to large particles (Fig. S2-S4) [66]. Micelle sizes formed by the P-GNGs were further investigated with detergent concentrations increasing from 0.4 to 1.0 wt% (Fig. 1c). Like DDM, most of the P-GNGs gave similar micelle sizes with increasing detergent concentration. The exceptions were GNG-3,11 and GNG-3,12 that showed reduced micelle sizes with increasing detergent concentration (Fig. 1c). Different from DDM, however, micelles formed by all P-GNGs were smallest at a detergent concentration of 1.0 wt% under the conditions tested. In contrast, OGNG micelles were substantially enlarged with increasing detergent concentration. Thus, micellar behaviors of the P-GNGs were different from those of the previous detergents (branch-chained maltosides and OGNG) [20,62].

3.2. Detergent evaluation with diverse membrane proteins

3.2.1. Detergent evaluation with AtBOR1—The P-GNGs were first evaluated with AtBOR1, expressed in *Saccharomyces cerevisiae* [49]. Protein stability in the individual detergents was initially assessed by monitoring the degree of protein unfolding during an 120-min incubation with a fluorescent dye (CPM) at 40 °C [51]. For this work, DDM-solubilized and purified AtBOR1 was diluted into buffer solutions containing the individual P-GNGs to give final detergent concentrations of CMCs+0.04 wt%. The thermal denaturation assay showed that OGNG was comparable to DDM in terms of maintaining the transporter in a folding state. All P-GNGs except GNG-1,12 and GNG-1,13 were better than the control detergents (DDM and OGNG) (Fig. 2 and S5). Detergent efficacy for AtBOR1 stability tended to improve with increasing pendant chain length; the P-GNGs with the propyl pendant were generally better than those with the methyl/ethyl pendant. A similar trend was observed when detergent concentrations were increased to CMCs+0.2 wt% (Fig. S6). Again, GNG-1,13 was just comparable to DDM/OGNG while the other P-GNGs were clearly more effective than the control detergents at preserving the folding state of the transporter. Based on the CPM results, we selected three P-GNGs, GNG-2,14, GNG-3,13 and GNG-3,14, for a FSEC study with the transporter. This methodology provides information on protein integrity and homogeneity. *S. cerevisiae* membranes containing AtBOR1-GFP fusion protein were incubated with the selected detergent at 1.0 wt%. All three selected P-GNGs and OGNG extracted the fusion protein as efficiently as DDM (Table S1). Protein stability in the selected detergents was assessed by measuring protein integrity *via* FSEC after a thermal treatment at 46 °C for 10 min. The detergent-extracted transporter gave rise to a monodisperse peak at about fraction 35 corresponding to the intact fusion protein (Fig. 2). In order to establish the oligomeric state of AtBOR1 solubilized in detergent, the molecular weight of the transporter purified in DDM was measured using size exclusion chromatography with multi-angle light scattering (SEC-MALS) and determined to be 176 ± 1 kDa (Fig. S7). This corresponds to the dimeric state of the protein. Based on a similar retention time in the FSEC profiles obtained in the P-GNGs and DDM, AtBOR1 solubilized in each P-GNG is also likely to be in the dimeric state, consistent with the known

structure of the protein [67]. Following thermal treatment, the intensity of this main peak was significantly reduced in the case of DDM, along with the appearance of a protein aggregation peak at about fraction 7 (Fig. 2c,d). Use of OGNG resulted in complete loss of the main peak and appearance of a large protein aggregation peak, indicating a much lower stability of the protein in this detergent than the other tested molecules. In contrast, upon heating the protein samples in the tested P-GNGs gave almost identical peaks to the unheated controls (Fig. 2 and S5b). The CPM and FSEC results led us to conclude that the selected P-GNGs (GNG-2,14, GNG-3,13 and GNG-3,14) are clearly superior to DDM/OGNG at maintaining AtBOR1 integrity.

3.2.2. Detergent evaluation with LeuT—The P-GNGs were further evaluated with the bacterial LeuT from *Aquifex aeolicus* [52]. The transporter was extracted from *E. coli* membranes using 1.0% DDM and purified in 0.05% of the same detergent. The DDM-purified LeuT was diluted with buffer solutions including the individual P-GNGs, OGNG, or DDM to give final detergent concentrations of CMCs+0.04 wt%. Protein stability was assessed by monitoring the ability of the transporter to bind a radio-labelled substrate ([^{3}H]-Leu) *via* SPA at regular intervals during a 11-day incubation at room temperature [53]. OGNG caused a complete loss of binding activity for the transporter after detergent exchange while DDM gave a gradual decrease in the ligand binding ability of the transporter over time (Fig. 3a). All P-GNGs except GNG-1,11 were comparable to or better than DDM at stabilizing the transporter, with the best performance observed for GNG-2,14. Similar results were observed for all P-GNGs when detergent concentration was increased to CMCs +0.2 wt% (Fig. 3b & S8). Once again, GNG-1,11 and GNG-2,14 were respectively the worst and the best of the P-GNGs. Representative P-GNGs (GNG-2,14, GNG-3,13 and GNG-3,14) were more effective than LMNG, a significantly optimized amphiphile, at stabilizing the transporter long term. The best performance was observed with GNG-2,14. Increasing detergent concentration from CMCs+0.04 to CMCs+0.2 wt% had little effect on detergent efficacy order for the most detergent cases, but the detergent efficacy of GNG-3,11 was substantially enhanced at the higher detergent concentration (Fig. 3b). With a few exceptions, we also observed the trend that the long alkyl chained P-GNGs are generally better than the short alkyl chained detergents at stabilizing the transporter. For instance, LeuT stability was enhanced with increasing main chain length for the methyl pendant-bearing GNGs (Fig. S8). P-GNG efficacy also tended to improve with increasing pendant chain length; the P-GNGs with the propyl pendant (GNG-3,11, GNG-3,12, GNG-3,13, and GNG-3,14) were notably better than the P-GNGs with the methyl/ethyl pendant except GNG-2,14 (Fig. 3a,b & S8).

3.2.3. Detergent evaluation with β_2AR—The encouraging results with AtBOR1 and LeuT prompted us to further evaluate the P-GNGs with a G protein-coupled receptor (GPCR), the human β_2AR [54]. DDM-purified receptor was diluted into buffer solutions supplemented with the individual P-GNGs to give final concentrations of CMCs+0.2 wt%. Receptor stability was assessed *via* ligand binding assay using a radio-active antagonist ([^{3}H]-DHA) [68,69]. A preliminary result was obtained by measuring the ligand binding ability of the receptor after 30-min dilution. DDM and OGNG-solubilized receptors gave respective high and low ligand binding capability (Fig. S9). As observed with LeuT,

detergent efficacy of the P-GNGs tended to be enhanced with increasing the main and/or pendant chain lengths. Consequently, GNG-1,14 and GNG-2,14 were the best P-GNGs with the methyl and ethyl pendants, respectively. In the case of the propyl pendant-bearing GNGs, all detergents except GNG-3,11 gave receptor activity as high as DDM. Based on this preliminary study, we selected five P-GNGs (GNG-1,14, GNG-2,14, GNG-3,12, GNG-3,13 and GNG-3,14) to measure receptor stability long term (Fig. 3c). GNG-1,14 was comparable to DDM whereas the other P-GNGs were better than this gold standard detergent for maintaining receptor activity long term, with the best performance observed for GNG-3,14 with the longest main and pendant chains.

3.2.4. Detergent evaluation with MelB—As for a further evaluation of the new detergents, we utilized the melibiose transporter (MelB) of *Salmonella typhimurium* [55-57,70,71]. *E. coli* membranes expressing $MelB_{St}$ were treated with 1.5 wt% of the individual P-GNGs, OGNG, or DDM for 90 min at 0 °C and the resulting detergent extracts were further incubated at 0 °C or an elevated temperature (45, 55, or 65 °C) for another 90 min. The amount of soluble $MelB_{St}$ was measured by SDS-PAGE and Western blotting after ultracentrifugation to remove insoluble fractions (Fig. 4a). Because of high $MelB_{St}$ stability at a low temperature, the amount of soluble $MelB_{St}$ detected at 0 °C is strongly correlated to detergent efficiency for protein extraction. Under the incubation at a higher temperature (45, 55, or 65 °C), however, $MelB_{St}$ would undergo protein aggregation, yielding different amounts of soluble $MelB_{St}$ depending on the abilities of individual detergents to stabilize the transporter. Thus, $MelB_{St}$ stability can be estimated based on the amount of soluble $MelB_{St}$ following the thermal treatments. All P-GNGs showed $MelB_{St}$ extraction efficiency comparable to DDM (Fig. 4a; 0 °C), indicating that this class of amphiphiles has the ability to effectively dismantle *E. coli* membranes. When detergent extracts were further incubated at 45 °C, two GNGs (OGNG and GNG-1,11) yielded only small amounts of soluble $MelB_{St}$ (20% and 40%, respectively); all the other detergents including DDM fully retained $MelB_{St}$ solubility under the conditions tested. A further increase in incubation temperature to 55 °C leads to large differentiation in detergent efficacy. The DDM-extracted $MelB_{St}$ completely aggregated during heat treatment, while three P-GNGs (GNG-2,14, GNG-3,13 and GNG-3,14) retained significant amounts of soluble $MelB_{St}$ under the same conditions (40, 30 and 70%, respectively). At 65 °C, none of the detergents was able to provide a detectable amount of soluble $MelB_{St}$.

To evaluate the functional state of soluble $MelB_{St}$, we tested GNG-3,14, the most effective at stabilizing $MelB_{St}$, utilizing Förster resonance energy transfer (FRET) from tryptophan (Trp) to the fluorescent ligand (D^2G) bound to the active site [57,72]. Upon addition of D^2G, functional MelB is highly fluorescent due to the occurrence of efficient FRET between Trp and bound D^2G. This high fluorescence intensity can be reversed upon addition of a sufficient amount of melibiose, a non-fluorescent substrate, due to the displacement of D^2G by melibiose in the active site. Thus, MelB functionality can be assessed by monitoring changes in fluorescence intensity of the transporter during sequential addition of D^2G and melibiose. DDM or GNG-3,14-extracted $MelB_{St}$ responded to addition of D^2G and melibiose, indicating that these protein samples are functional (Fig. 4b). When we used $MelB_{Ec}$, a less stable MelB homologue from *E. coli*, under the same conditions, DDM-

extracted transporter was not responsive to the addition of melibiose, indicating that DDM-extracted $MelB_{Ec}$ is not able to bind the sugar substrate. In contrast, GNG-3,14-extracted $MelB_{Ec}$ was functional under the same conditions. Thus, some P-GNGs, particularly GNG-3,14, were superior to DDM at maintaining the transporter in a soluble and functional state.

3.2.5. Detergent evaluation with MOR—As the three P-GNGs (GNG-2,14, GNG-3,13 and GNG-3,14) were significantly effective at stabilizing all four membrane proteins tested here (AtBOR1, LeuT, β_2AR and MelB), we selected these three P-GNGs for a further evaluation with another GPCR, the mouse MOR [73]. The receptor purified in 0.05% DDM and 0.005% CHS was incubated with buffer solutions containing 1.0 wt% GNG-2,14, GNG-3,13, or GNG-3,14 to obtain the detergent-exchanged receptor samples. Receptor stability was assessed by estimating melting temperature (T_m) via CPM assay at a detergent concentration of 0.5 wt% (Fig. 5a). T_m of the receptor solubilized in DDM was measured directly from the (DDM+CHS)-purified receptor without detergent exchange as the receptor was unstable in this conventional detergent. The receptor solubilized in [DDM +CHS] gave a low T_m of 31.6 °C (Table S2). In contrast, all tested P-GNGs resulted in receptor T_ms higher than DDM. The C14 alkyl chained GNGs (GNG-2,14 and GNG-3,14) gave receptor T_ms of ~ 41.0 °C, almost 10 °C higher than DDM. These GNGs were comparable to or better than LMNG (38.9 °C), a significantly optimized amphiphile that has had significant success with multiple transporters and GPCRs. Along with β_2AR result, this result indicates that these P-GNGs are likely useful for GPCR structural study.

3.2.6. Detergent evaluation with hENT1—The two C14 alkyl chained P-GNGs (GNG-2,14 and GNG-3,14) were further evaluated with hENT1 [74,75]. The transporter was extracted from the membrane using 1.0 wt% respective detergent. The two P-GNGs solubilized the transporter with similar efficiencies to DDM, consistent with the AtBOR1 and $MelB_{St}$ results (Fig. S10). Thermo-stability of the detergent-solubilized transporter was assessed using a radioactive ligand ([^{3}H]-NBMPR) following sample incubation at four different temperatures (4, 40, 45, or 50 °C) for 30 min [58,75]. DDM-solubilized hENT1 retained the ability to bind the ligand ([^{3}H]-NBMPR) after the 40 °C-incubation, but a further increase in incubation temperature to 45 °C resulted in a complete loss in ligand binding activity of the transporter (Fig. 5b). When GNG-2,14 or GNG-3,14 was used as a solubilizing agent, hENT1 showed two times higher activity than the transporter in DDM at a low temperature of 4 °C. Furthermore, the high protein activity was maintained up to 45 °C when the transporter was solubilized in each P-GNG, particularly in the case of GNG-3,14. This result indicates the superior behaviors of these P-GNGs in preserving the functional state of hENT1.

4. Discussion

We introduced here pendant-bearing detergents with a branched diglucoside headgroup and two different alkyl chains (long main and short pendant chains). These P-GNGs have a tendency to form small micelles compared to DDM and a previous GNG (OGNG) and showed little variation in micelle size with increasing detergent concentration. When the P-GNGs were tested with several membrane proteins (AtBOR1, LeuT, β_2AR, $MelB_{St}$, MOR

and hENT1), we found a general trend of detergent efficacy for protein stabilization. In most cases, the P-GNGs tended to give enhanced protein stability with the increase of the main and/or pendant chain lengths. Accordingly, the P-GNGs bearing the long main chain (C13/C14) and/or pendant chain (C2/C3) displayed favorable behaviors for membrane protein stabilization, with GNG-2,14, GNG-3,13, or GNG-3,14 being the most successful for all the membrane protein tested here. In contrast, GNG-1,11 with the shortest main and pendant chains appeared to be the least effective at stabilizing those membrane proteins. In addition, analysis of AtBOR1, $MelB_{St}$ and hENT1 solubilization indicates that these detergents are as efficient as DDM and OGNG at extracting membrane proteins from the membranes. As OGNG was shown to be compatible with *in surfo*-based protein crystallization [42-46], these three P-GNGs will be useful for membrane protein structural study. Data shows that the three P-GNGs identified here (GNG-2,14, GNG-3,13 and GNG-3,14) could be favorably used in several steps including protein extraction, solubilization, stabilization and crystallization. The behaviors of GNG-2,14 and GNG-3,14 are particularly remarkable as these GNGs were comparable to or even better than LMNG for LeuT and MOR stability. This result is in contrast to the general notion that glucoside detergents are substantially inferior to maltoside detergents (e.g., OG vs DDM) at stabilizing membrane proteins.

It is important to understand why the P-GNGs were superior to the previous GNG (OGNG) for membrane protein stabilization [20]. The hydrophobic length of this original GNG is too short (hexyl; C6) to be compatible with the hydrophobic widths of membrane proteins (28-32 Å). Our previous attempt to increase the chain lengths of both alkyl groups together (e.g., GNG-7,7) was unsuccessful due to the limited water-solubility of these versions (<1.0 wt%). In this study, we solved this issue by incorporating alkyl groups of differing chain length and the resulting P-GNGs were highly water-soluble even when main and pendant chain lengths of C14 and C3, respectively, were used. The best efficacy of two C14 alkyl chained P-GNGs (GNG-2,14 and GNG-3,14) indicates that the C14 chain length is optimal for protein stabilization. Detergent efficacy for protein stabilization was further optimized by introducing the propyl pendant (e.g., GNG-3,14 *vs* GNG-1,14) in the hydrophilic-hydrophobic interfaces of detergent micelles, suggesting an important role of this pendant chain in protein stability. As micelle sizes of the P-GNGs were invariant with increasing pendant chain length from C1 (methyl) to C3 (propyl) (Table 1 & Fig. 1), these additional chains (methyl, ethyl, or propyl) seem well accommodated in empty micellar spaces produced by single alkyl chained GNGs (hypothetical monopod GNG; Fig. 6). Consequently, the additional presence of the pendant chain, particularly the propyl chain, increases alkyl chain density in the micelle interiors compared to those formed by the monopod GNG and accordingly strengthens hydrophobic interactions between the detergent alkyl chains, resulting in enhanced micellar stability. The high micellar stability of the propyl pendant-bearing GNGs is supported by their low CMCs and high water-solubility. Due to the presence of the relatively large head group compared to the hydrophobic group, a monopod GNG might be better than the P-GNGs at preventing protein denaturation (Fig. 6). However, a single alkyl chained GNG is likely to have reduced binding affinity to the hydrophobic surfaces of membrane proteins, which in turn could induce significant protein aggregation. As membrane proteins are known to lose their function via two main mechanisms, denaturation and aggregation, it is important to effectively prevent protein

aggregation as well as denaturation to achieve enhanced protein stability. This indicates that a detergent needs to have an appropriate hydrophilic-lipophilic balance (HLB), in order to confer membrane protein stability. Due to the presence of the pendant (the ethyl or propyl chain) in the hydrophilic-hydrophobic interfaces, micelles formed by the P-GNGs have increased hydrophobic interactions between detergent molecules, leading to more stable micelles. This in turn leads to effective encapsulation of membrane proteins and thus low levels of protein aggregation. In addition, the large differences in chain length between the main and pendant chains imply that these P-GNGs, like a monopod GNG, would cause little protein denaturation. Thus, the ethyl or propyl pendant-bearing GNGs are not only effective at preventing protein aggregation, but also at alleviating protein denaturation, providing an explanation for their enhanced protein stabilization efficacy observed here. The previously developed GNGs, are likely to form micelles with an elliptical rather than spherical shape given their approximate cylindrical shape, as indicated by the large micelle size (R_h = 4.46 nm) (Fig. 6). Due to the presence of two short and identical alkyl chains, the previous GNGs are unlikely to pack tightly in either micelles or PDCs, resulting in micelle instability. Their relatively high CMCs (e.g., 1.0 mM (OGNG)) and poor water-solubility (e.g., GNG-7,7) are indications of their limited micellar stability. Collectively, the main alkyl chains of the P-GNGs dictate the detergent hydrophobic length that needs to be compatible with the protein hydrophobic widths, while their pendant chains have a significant role in enhancing micelle/protein stability. The current study first introduced the independent roles of detergent two alkyl chains in protein stabilizations and thus provides a new avenue to develop future detergents for membrane protein study.

A previous study showed that branch-chained DDM analogues with pendant chains similar to those of the P-GNGs failed to give enhanced protein stability compared to DDM [62]. The P-GNGs described in the current study contain branched diglucoside head groups larger than the maltoside of the branch-chained DDM analogues. Thus, unlike the maltoside detergents, the single-chained GNGs produce large empty spaces in the micelle interiors that can be effectively filled by the pendant chains (ethyl or propyl chains) introduced by the P-GNGs. This is supported by the finding that the micelle sizes of the new GNGs were independent of pendant chain length. In contrast, micelles were substantially enlarged with the same variation of the branch-chained DDM analogues. This comparison indicates that the short branches in the previous DDM analogues are unlikely to be effective at increasing alkyl chain density/hydrophobic interactions within micelles. Thus, it is important to consider the relative volume of detergent head and tail groups in order to understand whether the introduction of a pendant chain favors protein stability. At this point, it is unclear which length of a pendant chain in the P-GNG scaffold would be optimal for protein stability. A further increase in the pendant chain length could further improve detergent property, a feature which is currently under investigation.

5. Conclusions

By introducing main and pendant chains into the previous GNG scaffold, we prepared twelve P-GNGs that have a tendency to form compact micelles compared to DDM and OGNG. In evaluation of these detergents with several membrane proteins, we identified three detergents (GNG-2,14, GNG-3,13 and GNG-3,14) more suitable for membrane protein

stabilization than DDM and OGNG. Detergent efficacy of the P-GNGs for protein stabilization was optimized by both varying the main chain length and introducing the pendant chains such as ethyl and propyl chains in the hydrophobic-hydrophilic interface. These pendant-bearing GNGs possess the same head group as OGNG (i.e., branched diglucoside) that has proved effective for structure determinations of membrane proteins. Moreover, the current data shows that they are successful in different steps such as protein extraction and stabilization, strongly suggesting that these pendant-bearing GNGs hold significant potential in membrane protein structural study. Introduction of pendant chains in the empty spaces of detergent micelles represents a conceptual advance of detergent design in membrane protein study.

Supplementary Material

Refer to Web version on PubMed Central for supplementary material.

Acknowledgements

This work was supported by the National Research Foundation of Korea (NRF) (grant numbers 2016R1A2B2011257, 2018R1A6A1A03024231 to P.S.C.), *National Institutes of Health (NIH)* Awards (grant numbers R01GM122759, R21NS105863 to L.G), and Japan Society for the Promotion of Science (JSPS) award (Grant-in-Aid for JSPS Fellows 17J03042 to S.K.). D^2G was obtained from Drs. Gerard Leblanc and H. Ronald Kaback.

References

1. Drake MT, Shenoy SK, Lefkowitz RJ, Trafficking of G Protein–Coupled Receptors, Circ. Res 99 (2006) 570–582. [PubMed: 16973913]
2. Lappano R, Maggiolini M, G protein-coupled receptors: novel targets for drug discovery in cancer, Nat. Rev. Drug Discovery 10 (2011) 47–60. [PubMed: 21193867]
3. Santos R, Ursu O, Gaulton A, Bento AP, Donadi RS, Bologa CG, Karlsson A, Al-Lazikani B, Hersey A, Oprea TI, Overington JP, A comprehensive map of molecular drug targets, Nat. Rev. Drug discovery 16 (2017) 19–34. [PubMed: 27910877]
4. White SH, Wimley WC, Membrane protein folding and stability: physical principles, Annu. Rev. Biophys. Biomol. Struct 28 (1999) 319–365. [PubMed: 10410805]
5. Møller JV, le Maire M, Detergent binding as a measure of hydrophobic surface area of integral membrane proteins, J. Biol. Chem 268 (1993) 18659–18672. [PubMed: 8395515]
6. Serrano-Vega MJ, Magnani F, Shibata Y, Tate CG, Conformational thermostabilization of the β1-adrenergic receptor in a detergent-resistant form, Proc. Natl. Acad. Sci. U. S. A 105 (2008) 877–882. [PubMed: 18192400]
7. Newstead S, Ferrandon S, Iwata S, Rationalizing α-helical membrane protein crystallization, Protein Sci. 17 (2008) 466–472. [PubMed: 18218713]
8. He Y, Wang K, Yan N, The recombinant expression systems for structure determination of eukaryotic membrane proteins, Protein Cell. 5 (2014) 658–672. [PubMed: 25119489]
9. https://www.wwpdb.org/
10. Newstead S, Hobbs J, Jordan D, Carpenter EP, Iwata S, Insights into outer membrane protein crystallization, Mol. Membr. Biol 25 (2008) 631–638. [PubMed: 19023694]
11. Garavito RM, Ferguson-Miller S, Detergents as tools in membrane biochemistry, J. Biol. Chem 276 (2001) 32403–32406. [PubMed: 11432878]
12. Bowie JU, Stabilizing membrane proteins, Curr. Opin. Struct. Biol 11 (2001) 397–402. [PubMed: 11495729]
13. Lacapére JJ, Pebay-Peyroula E, Neumann JM, Etchebest C, Determining membrane protein structures: still a challenge!, Trends Biochem. Sci 32 (2007) 259–270. [PubMed: 17481903]

14. McGregor C-L, Chen L, Pomroy NC, Hwang P, Go S, Chakrabartty A, Privé GG, Lipopeptide detergents designed for the structural study of membrane proteins, Nat. Biotechnol 21 (2003) 171–176. [PubMed: 12524549]
15. Nath A, Atkins WM, Sligar SG, Applications of phospholipid bilayer nanodiscs in the study of membranes and membrane proteins, Biochemistry 46 (2007) 2059–2069. [PubMed: 17263563]
16. Tao H, Lee SC, Moeller A, Roy RS, Siu FY, Zimmermann J, Stevens RC, Potter CS, Carragher B, Zhang Q, Engineered nanostructured β-sheet peptides protect membrane proteins, Nat. Methods 10 (2013) 759–761. [PubMed: 23817067]
17. Tribet C, Audebert R, Popot J-L, Amphipols: polymers that keep membrane proteins soluble in aqueous solutions, Proc. Natl. Acad. Sci. U.S.A 93 (1996) 15047–15050. [PubMed: 8986761]
18. Popot JL, Althoff T, Bagnard D, Banères JL, Bazzacco P, Billon-Denis E, Catoire LJ, Champeil P, Charvolin D, Cocco MJ, Crèmel G, Dahmane T, de la Maza LM, Ebel C, Gabel F, Giusti F, Gohon Y, Goormaghtigh E, Guittet E, Kleinschmidt JH, Kuhlbrandt W, Le Bon C, Martinez KL, Picard M, Pucci B, Sachs JN, Tribet C, van Heijenoort C, Wien F, Zito F, Zoonens M, Amphipols from A to Z, Annu. Rev. Biophys 40 (2011) 379–408. [PubMed: 21545287]
19. Dörr JM, Scheidelaar S, Koorengevel MC, Dominguez JJ, Schäfer M, van Walree CA, Killian JA, The styrene–maleic acid copolymer: a versatile tool in membrane research, Eur. Biophys. J 45 (2016) 3–21. [PubMed: 26639665]
20. Chae PS, Rana RR, Gotfryd K, Rasmussen SGF, Kruse AC, Cho KH, Capaldi S, Carlsso E, Kobilka B, Loland CJ, Gether U, Banerjee S, Byrne B, Lee JK, Gellman SH, Glucose-neopentyl glycol (GNG) amphiphiles for membrane protein study, Chem. Commun 49 (2013) 2287–2289.
21. Chae PS, Rasmussen SGF, Rana RR, Gotfryd K, Chandra R, Goren MA, Kruse AC, Nurva S, Loland CJ, Pierre Y, Drew D, Popot JL, Picot D, Fox BG, Guan L, Gether U, Byrne B, Kobilka B, Gellman SH, Maltose–neopentyl glycol (MNG) amphiphiles for solubilization, stabilization and crystallization of membrane proteins, Nat. Methods 7 (2010) 1003–1008. [PubMed: 21037590]
22. Sadaf A, Mortensen JS, Capaldi S, Tikhonova E, Hariharan P, Ribeiro O, Loland CJ, Guan L, Byrne B, Chae PS, A class of rigid linker-bearing glucosides for membrane protein structural study, Chem. Sci 7 (2016) 1933–1939. [PubMed: 27110345]
23. Hussain H, Du Y, Scull NJ, Mortensen JS, Tarrasch J, Loland CJ, Byrne B, Kobilka BK, Chae PS, Accessible Mannitol-Based Amphiphiles (MNAs) for Membrane Protein Solubilisation and Stabilisation, Chem.–Eur. J 22 (2016) 7068–7073. [PubMed: 27072057]
24. Hussain H, Du Y, Tikhonova E, Mortensen JS, Ribeiro O, Santillan C, Das M, Ehsan M, Loland CJ, Guan L, Kobilka BK, Byre B, Chae PS, Resorcinarene-Based Facial Glycosides: Implication of Detergent Flexibility on Membrane-Protein Stability, Chem.–Eur. J 23 (2017) 6724–6729 [PubMed: 28303608]
25. Ehsan M, Du Y, Scull NJ, Tikhonova E, Tarrasch J, Mortensen JS, Loland CJ, Skiniotis G, Guan L, Byrne B, Kobilka B, Chae PS, Highly branched pentasaccharide-bearing amphiphiles for membrane protein studies, J. Am. Chem. Soc 138 (2016) 3789–3796. [PubMed: 26966956]
26. Sadaf A, Du Y, Santillan C, Mortensen JS, Molist I, Seven AB, Hariharan P, Skiniotis G, Loland CJ, Kobilka BK Guan L, Byrne B, Chae PS, Dendronic trimaltose amphiphiles (DTMs) for membrane protein study, Chem. Sci 8 (2017) 8315–8324. [PubMed: 29619178]
27. Das M, Du Y, Mortensen JS, Ribeiro O, Hariharan P, Guan L, Loland CJ, Kobilka BK, Byrne B, Chae PS, Butane-1, 2, 3, 4-tetraol-based amphiphilic stereoisomers for membrane protein study: importance of chirality in the linker region, Chem. Sci 8 (2017) 1169–1177. [PubMed: 28451257]
28. Das M, Du Y, Ribeiro O, Hariharan P, Mortensen JS, Patra D, Skiniotis G, Loland CJ, Guan L, Kobilka BK, Byrne B, Chae PS, Conformationally preorganized diastereomeric norbornane-based maltosides for membrane protein study: Implications of detergent kink for micellar properties, J. Am. Chem. Soc 139 (2017) 3072–3081. [PubMed: 28218862]
29. Rosenbaum DM, Zhang C, Lyons J, Holl R, Aragao D, Arlow DH, Rasmussen SGF, Choi HJ, DeVree BT, Sunahara RK, Chae PS, Gellman SH, Dror RO, Shaw DE, Weis WI, Caffrey M, Gmeiner P, Kobilka BK, Structure and function of an irreversible agonist-β 2 adrenoceptor complex, Nature 469 (2011) 236–240. [PubMed: 21228876]

30. Haga K, Kruse AC, Asada H, Kobayashi TY, Shiroishi M, Zhang C, Weis WI, Okada T, Kobilka BK, Haga T, Kobayashi T, Structure of the human M2 muscarinic acetylcholine receptor bound to an antagonist, Nature. 482 (2012) 547–551. [PubMed: 22278061]

31. Kruse AC, Ring AM, Manglik A, Hu J, Hu K, Eitel K, Hubner H, Pardon E, Valant C, Sexton PM, Christopoulos A, Felder CC, Gmeiner P, Steyaert J, Weis WI, Garcia KC, Wess J, Kobilka BK, Activation and allosteric modulation of a muscarinic acetylcholine receptor, Nature 504 (2013) 101–106. [PubMed: 24256733]

32. Dickson VK, Pedi L, Long SB, Structure and insights into the function of a Ca^{2+}-activated Cl^{-} channel, Nature, 516 (2014) 213–218. [PubMed: 25337878]

33. Yin J, Mobarec JC, Kolb P, Rosenbaum DM, Crystal structure of the human OX 2 orexin receptor bound to the insomnia drug suvorexant, Nature 519 (2015) 247–250 [PubMed: 25533960]

34. Perez C, Gerber S, Boilevin J, Bucher M, Darbre T, Aebi M, Reymond JL, Locher KP, Structure and mechanism of an active lipid-linked oligosaccharide flippase, Nature 524 (2015) 433–438. [PubMed: 26266984]

35. Paulsen CE, Jean-Paul A, Gao Y, Cheng Y, Julius D, Structure of the TRPA1 ion channel suggests regulatory mechanisms, Nature 520 (2015) 511–517. [PubMed: 25855297]

36. Schmidt HR, Zheng S, Gurpinar E, Koehl A, Manglik A, Kruse AC, Crystal structure of the human σ 1 receptor, Nature 532 (2016) 527–530. [PubMed: 27042935]

37. Zhang Z, Chen J, Atomic structure of the cystic fibrosis transmembrane conductance regulator, Cell 167 (2016) 1586–1597. [PubMed: 27912062]

38. Liang Y-L, Khoshouei M, Radjainia M, Zhang Y, Glukhova A, Tarrasch J, Thal DM, Furness SGB, Christopoulos G, Coudrat T, Danev R, Baumeister W, Miller LJ, Christopoulos A, Kobilka BK, Wootten D, Skiniotis G, Sexton PM, Phase-plate cryo-EM structure of a class B GPCR–G-protein complex, Nature 546 (2017) 118–123. [PubMed: 28437792]

39. Glukhova A, Thal DM, Nguyen AT, Vecchio EA, Jörg M, Scammells PJ, May LT, Sexton PM, Christopoulos A, Structure of the adenosine A1 receptor reveals the basis for subtype selectivity. Cell 168 (2017) 867–877. [PubMed: 28235198]

40. Caffrey M, Li D, Dukkipati A, Membrane protein structure determination using crystallography and lipidic mesophases: recent advances and successes, Biochemistry 51 (2012) 6266–6288. [PubMed: 22783824]

41. Urner LH, Liko I, Yen H-Y, Hoi K-K, Bolla JR, Gault J, Almeida FG, Schweder M-P, Shutin D, Ehrmann S, Haag R, Robinson CV, Pagel K, Modular detergents tailor the purification and structural analysis of membrane proteins including G-protein coupled receptors, Nat. Commun 11 (2020) 564. [PubMed: 31992701]

42. Kellosalo J, Kajander T, Kogan K, Pokharel K, Goldman A, The structure and catalytic cycle of a sodium-pumping pyrophosphatase, Science 337 (2012) 473–476. [PubMed: 22837527]

43. Quigley A, Dong YY, Pike ACW, Dong L, Shrestha L, Berridge G, Stansfeld PJ, Sansom MSP, Edwards AM, Bountra C, von Delft F, Bullock AN, Burgess-Brown NA, Carpenter EP, The structural basis of ZMPSTE24-dependent laminopathies, Science 339 (2013) 1604–1607. [PubMed: 23539603]

44. Frick A, Eriksson UK, de Mattia F, Öberg F, Hedfalk K, Neutze R, de Grip WJ, Deen PMT, Tornroth-Horsefield S, X-ray structure of human aquaporin 2 and its implications for nephrogenic diabetes insipidus and trafficking, Proc. Natl. Acad. Sci. U.S.A 111 (2014) 6305–6310. [PubMed: 24733887]

45. Karakas E, Furukawa H, Crystal structure of a heterotetrameric NMDA receptor ion channel, Science 344 (2014) 992–997. [PubMed: 24876489]

46. Dong YY, Pike ACW, Mackenzie A, McClenaghan C, Aryal P, Dong L, Quigley A, Grieben M, Goubin S, Mukhopadhyay S, Ruda GF, Clausen MV, Cao LS, Brennan PE, Burgess-Brown NA, Sansom MSP, Tucker SJ, Carpenter EP, K2P channel gating mechanisms revealed by structures of TREK-2 and a complex with Prozac, Science 347 (2015) 1256–1259. [PubMed: 25766236]

47. Kunji ER, Harding M, Butler PJ, Akamine P, Determination of the molecular mass and dimensions of membrane proteins by size exclusion chromatography, Methods 46 (2008) 62–72. [PubMed: 18952172]

48. Zhang Q, Tao H, Hong WX, New amphiphiles for membrane protein structural biology, Methods 55 (2011) 318–323. [PubMed: 21958988]
49. Drew D, Newstead S, Sonoda Y, Kim H, von Heijne G, Iwata S, GFP-based optimization scheme for the overexpression and purification of eukaryotic membrane proteins in *Saccharomyces cerevisiae*, Nat. Protoc 3 (2008) 784–798. [PubMed: 18451787]
50. Leung J, Karachaliou M, Alves C, Diallinas G, Byrne B, Stabilizing the heterologously expressed uric acid-xanthine transporter UapA from the lower eukaryote *Aspergillus nidulans*, Protein Expr. Purif 72 (2010) 139–146. [PubMed: 20153431]
51. Alexandrov A, Mileni M, Chien EYT, Hanson MA, Stevens RC, Microscale fluorescent thermal stability assay for membrane proteins, Structure 16 (2008) 351–359. [PubMed: 18334210]
52. Deckert G, Warren PV, Gaasterland T, Young WG, Lenox AL, Graham DE, Overbeek R, Snead MA, Keller M, Aujay M, Huber R, Feldman RA, Short JM, Olsen GJ, Swanson RV, The complete genome of the hyperthermophilic bacterium *Aquifex aeolicus*, Nature 392 (1998) 353–358. [PubMed: 9537320]
53. Quick M, Javitch JA, Monitoring the function of membrane transport proteins in detergent-solubilized form, Proc. Natl. Acad. Sci. U.S.A 104 (2007) 3603–3608. [PubMed: 17360689]
54. Rosenbaum DM, Cherezov V, Hanson MA, Rasmussen SG, Thian FS, Kobilka TS, Choi HJ, Yao XJ, Weis WI, Stevens RC, Bobilka BK, GPCR engineering yields high-resolution structural insights into β2-adrenergic receptor function, Science 318 (2007) 1266–1273. [PubMed: 17962519]
55. Pourcher T, Leclercq S, Brandolin G, Leblanc G, Melibiose permease of Escherichia coli: Large scale purification and evidence that H^+, Na^+, and Li^+ sugar symport is catalyzed by a single polypeptide, Biochemistry 34 (1995) 4412–4420. [PubMed: 7703254]
56. Guan L, Nurva S, Ankeshwarapu SP, Mechanism of melibiose/cation symport of the melibiose permease of *Salmonella typhimurium*, J. Biol. Chem 286 (2011) 6367–6374. [PubMed: 21148559]
57. Maehrel C, Cordat E, Mus-Veteau I, Leblanc G, Structural Studies of the Melibiose Permease of *Escherichia coli* by Fluorescence Resonance Energy Transfer I. EVIDENCE FOR ION-INDUCED CONFORMATIONAL CHANGE, J. Biol. Chem 273 (1998) 33192–33197. [PubMed: 9837887]
58. Rehan S, Jaakola VP, Expression, purification and functional characterization of human equilibrative nucleoside transporter subtype-1 (hENT1) protein from Sf9 insect cells, Protein Expr. Purif 114 (2015) 99–107. [PubMed: 26162242]
59. Rehan S, Paavilainen VO, Jaakola VP, Functional reconstitution of human equilibrative nucleoside transporter-1 into styrene maleic acid co-polymer lipid particles, Biochim. Biophys. Acta-Biomembr 1859 (2017) 1059–1065. [PubMed: 28254415]
60. Cho KH, Hariharan P, Mortensen JS, Du Y, Nielsen AK, Byrne B, Kobilka BK, Loland CJ, Guan L, Chae PS, Isomeric Detergent Comparison for Membrane Protein Stability: Importance of Inter-Alkyl-Chain Distance and Alkyl Chain Length, ChemBioChem 17 (2016) 2334–2339. [PubMed: 27981750]
61. Chae PS, Kruse AC, Gotfryd K, Rana RR, Cho KH, Rasmussen SGF, Bae HE, Gether U, Guan L, Loland CJ, Byrne B, Kobilka BK, Gellman SH, Novel tripod amphiphiles for membrane protein analysis, Chem.–Eur. J 19 (2013) 15645–15651. [PubMed: 24123610]
62. Hong WX, Baker KA, Ma X, Stevens RC, Yeager M, Zhang Q, Design, synthesis, and properties of branch-chained maltoside detergents for stabilization and crystallization of integral membrane proteins: human connexin 26, Langmuir 26 (2010) 8690–8696. [PubMed: 20232919]
63. Bae HE, Du Y, Hariharan P, Mortensen JS, Kumar KK, Ha B, Das M, Lee HS, Loland CJ, Guan L, Kobilka BK, Chae PS, Asymmetric maltose neopentyl glycol amphiphiles for a membrane protein study: effect of detergent asymmetricity on protein stability, Chem. Sci 10 (2019) 1107–1116. [PubMed: 30774908]
64. Chattopadhyay A, London E, Fluorimetric determination of critical micelle concentration avoiding interference from detergent charge, Anal. Biochem 139 (1984) 408–412. [PubMed: 6476378]
65. Israelachvili J, Mitchell DJ, Ninham BW, Theory of self-assembly of hydrocarbon amphiphiles into micelles and bilayers, J. Chem. Soc., Faraday Trans. 2 72 (1976) 1525–1568.
66. Plum MA, Steffen W, Fytas G, Knoll W, Menges B, Probing dynamics at interfaces: resonance enhanced dynamic light scattering, Opt. Express 17 (2009) 10364–10371. [PubMed: 19506690]

67. Thurtle-Schmidt BH, Stroud RM, Structure of Bor1 supports an elevator transport mechanism for SLC4 anion exchangers, Proc. Natl. Acad. Sci. U.S.A 113 (2016) 10542–10546. [PubMed: 27601653]

68. Yao X, Parnot C, Deupi X, Ratnala VRP, Swaminath G, Farrens D, Kobilka B, Coupling ligand structure to specific conformational switches in the β2-adrenoceptor, Nat. Chem. Biol 2 (2006) 417–422. [PubMed: 16799554]

69. Swaminath G, Steenhuis J, Kobilka BK, Lee TW, Allosteric modulation of β2-adrenergic receptor by Zn^{2+}, Mol. Pharmacol 61 (2002) 65–72. [PubMed: 11752207]

70. Ethayathulla AS, Yousef MS, Amin A, Leblanc G, Kaback HR, Guan L, Structure-based mechanism for Na+/melibiose symport by MelB, Nat. Commun 5 (2014) 3009. [PubMed: 24389923]

71. Hariharan P, Guan L, Thermodynamic cooperativity of cosubstrate binding and cation selectivity of *Salmonella typhimurium* MelB, J. Gen. Physiol 149 (2017) 1029–1039. [PubMed: 29054867]

72. Amin A, Hariharan P, Chae PS, Guan L, Effect of detergents on galactoside binding by Melibiose permeases, Biochemistry 54 (2015) 5849–5855. [PubMed: 26352464]

73. Manglik A, Kruse AC, Kobilka TS, Thian FS, Mathiesen JM, Sunahara RK, Pardo L, Weis WI, Kobilka BK, Granier S, Crystal structure of the μ-opioid receptor bound to a morphinan antagonist, Nature 485 (2012) 321–326. [PubMed: 22437502]

74. Li RW, Yang C, Sit AS, Lin SY, Ho EY, Leung GP, Physiological and pharmacological roles of vascular nucleoside transporters, J. Cardiovasc. Pharmacol 59 (2012) 10–15. [PubMed: 21266914]

75. Chow L, Lai R, Dabbagh L, Belch A, Young JD, Cass CE, Mackey JR, Analysis of human equilibrative nucleoside transporter 1 (hENT1) protein in non-Hodgkin's lymphoma by immunohistochemistry, Mod. Pathol 18 (2005) 558–564. [PubMed: 15529184]

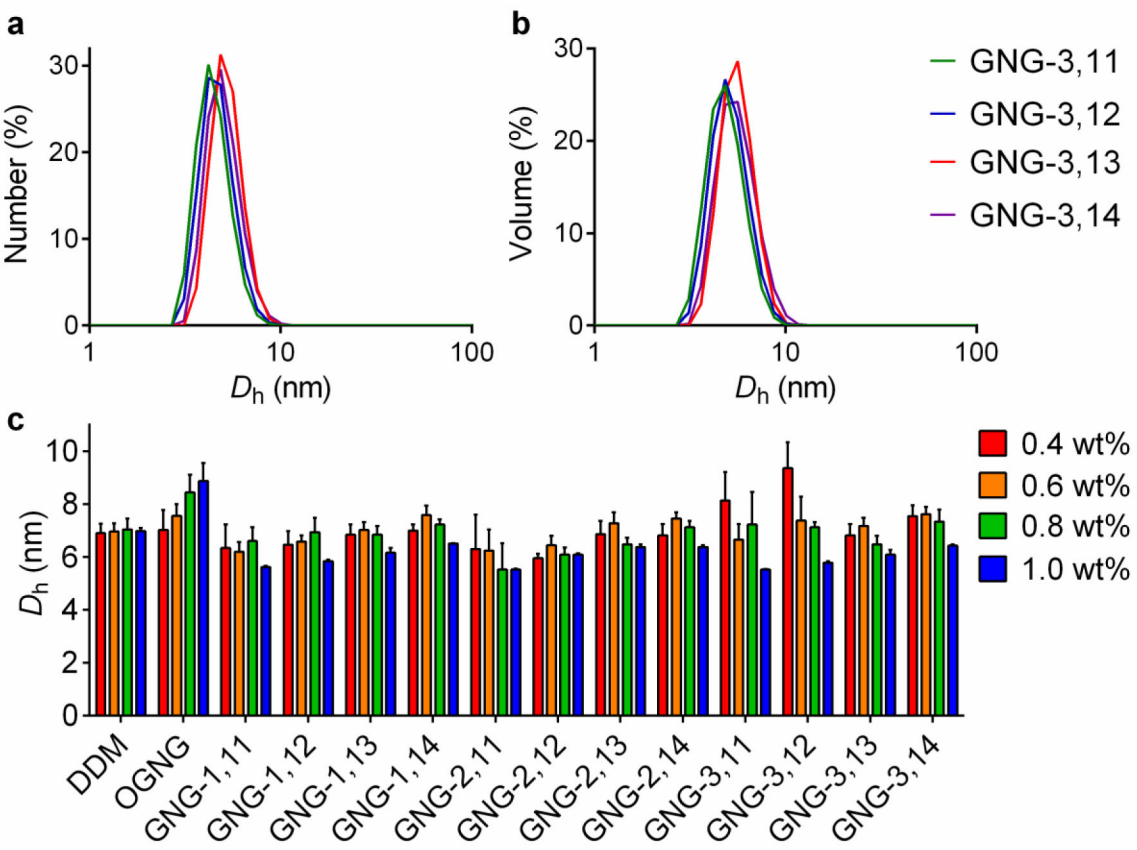

Figure 1.

(a,b) Number- and volume-weighted dynamic light scattering (DLS) profiles of detergent micelles formed by propyl pendant-bearing GNGs (GNG-3,11, GNG-3,12, GNG-3,13 and GNG-3,14) and (c) detergent concentration-dependent size variation of micelles formed by P-GNGs. The DLS profiles were obtained using 1.0 wt% P-GNGs (a,b), while detergent concentration varied from 0.4 to 1.0 wt% at room temperature (c). Detergent micelle size was represented by hydrodynamic diameter (D_h). OGNG and DDM were used as control detergents in the detergent concentration-dependent experiment for comparison. Error bars, SEM, $n = 5$.

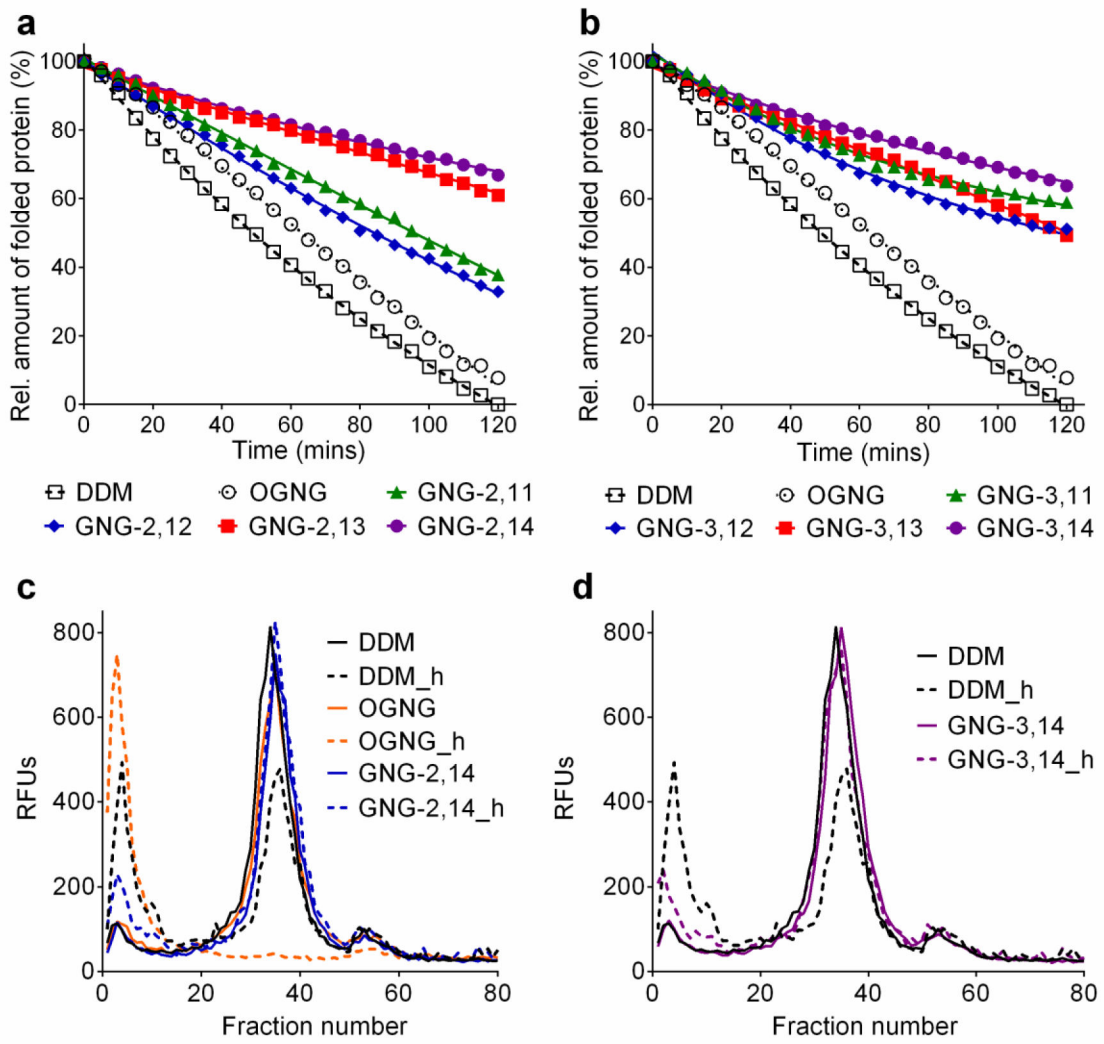

Figure 2.

(a,b)Thermal denaturation profiles of AtBOR1 in individual P-GNGs and (c,d) fluorescence size exclusion chromatography (FSEC) traces of AtBOR1-GFP fusion protein in the selected P-GNGs (GNG-2,14 and GNG-3,14). DDM and OGNG were used as control detergents. Thermal stability of the transporter was monitored by CPM assay performed at 40°C for 120 min at detergent concentrations of CMCs+0.04 wt%. The relative amounts of folded protein were normalized relative to the most destabilizing condition, which was obtained from the use of DDM in this experiment. FSEC traces were obtained after a heat treatment of detergent-solubilized AtBOR1-GFP for 10 min at 46 °C prior to loading onto the SEC column. The void volume was ~7 mL corresponding to fraction 7. The data shown is representative of two independent experiments. ‘h’ on the detergent label represents the heat-treated sample.

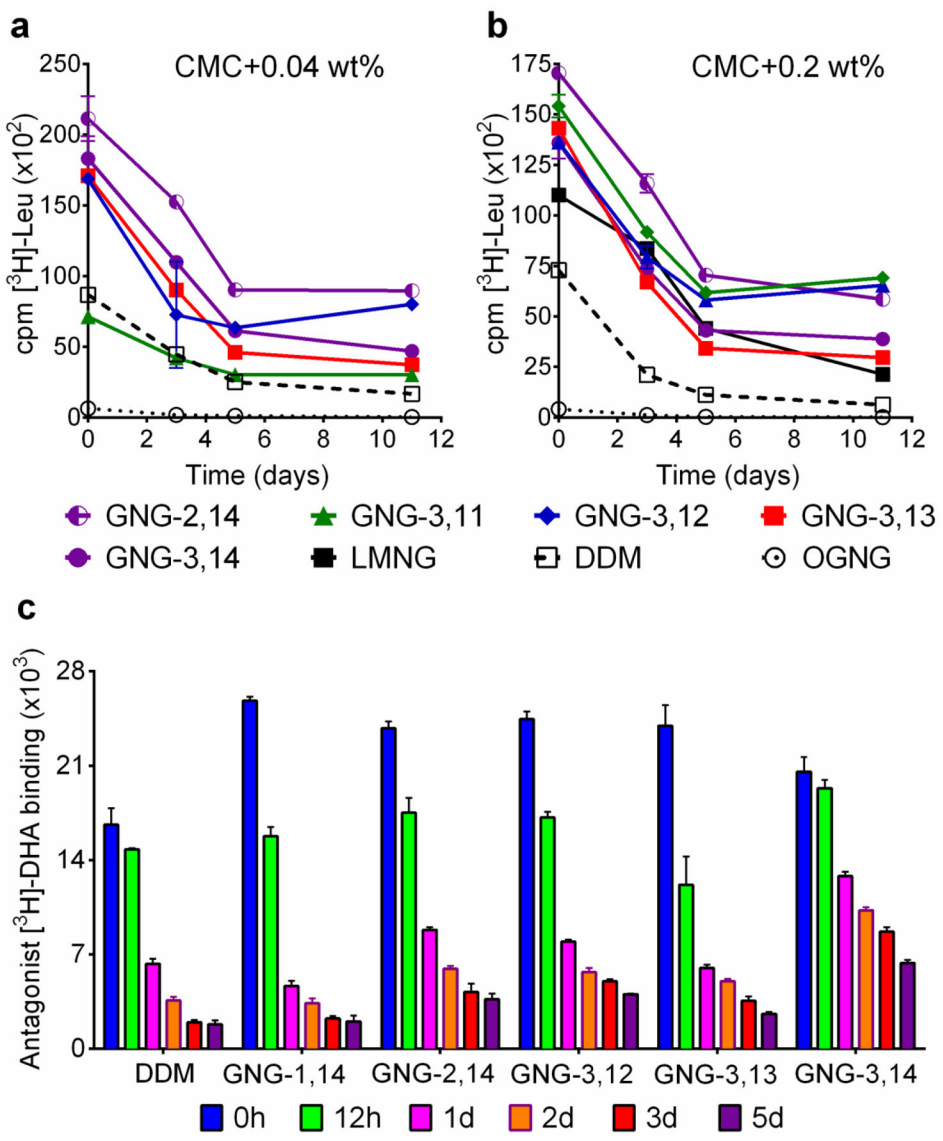

Figure 3.

Effect of P-GNGs on LeuT (a,b) and β_2AR stability (c). DDM or OGNG was used as a control. As for LeuT stability assay, DDM-purified transporter was diluted into a buffer containing a new GNG (GNG-2,14, GNG-3,11, GNG-3,12, GNG-3,13, or GNG-3,14), DDM, or OGNG at CMCs + 0.04 wt% (a) and CMCs + 0.2 wt% (b). LMNG was included as a control for detergent evaluation at CMCs + 0.2 wt%. For β_2AR stability analysis, DDM-purified receptor was diluted into a buffer containing a representative P-GNG (GNG-1,14, GNG-2,14, GNG-3,12, GNG-3,13, or GNG-3,14) at CMCs + 0.2 wt% (c). LeuT activity was assessed by monitoring [^{3}H]-leucine (Leu) binding capability via the scintillation proximity assay (SPA) at designated time points over a 11-day incubation period at room temperature. β_2AR stability was assessed by measuring ligand binding ability using the radiolabeled antagonist ([^{3}H]-dihydroalprenolol (DHA)) following 30-min dilution (0 h) and further monitoring receptor activity at regular intervals during a 5-day incubation at room temperature. Data points are means ± SEM (error bars); n = 2-3 (LeuT) or n = 3 (β_2AR).

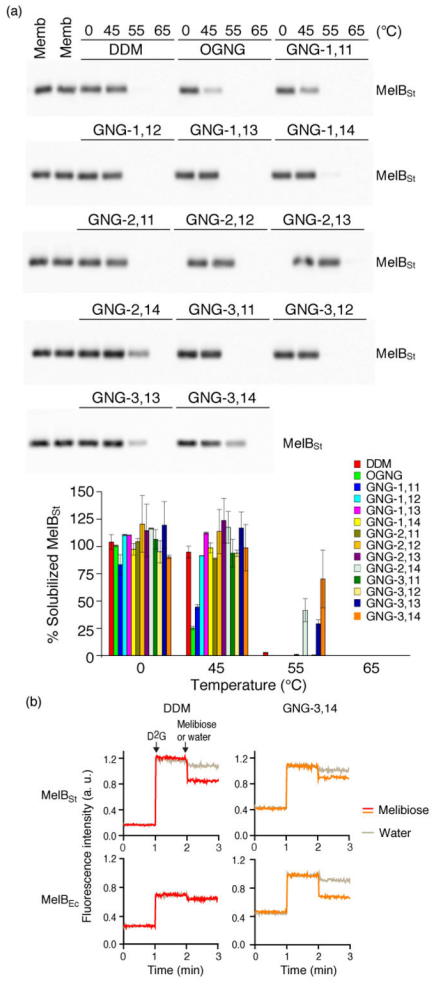

Figure 4.

(a) Thermo-stability of $MelB_{St}$ solubilized in P-GNGs. DDM and OGNG were used as control detergents. *E. coli* membranes containing $MelB_{St}$ were incubated with 1.5 wt% individual detergents for 90 min at 0 °C and $MelB_{St}$ extracts were further incubated at 0 °C or an elevated temperature (45, 55, or 65 °C) for 90 min. The amounts of soluble $MelB_{St}$ extracted by the individual detergents were analysed by SDS-PAGE and Western blotting (top panel) after ultracentrifugation as described in Materials and Methods. The amount of soluble $MelB_{St}$ in each sample was estimated from gel image analysis and expressed as a percentage of the total amount of $MelB_{St}$ in the untreated membrane ('Memb') in the histogram (bottom panel). Error bars, SEM; $n = 2$. (b) MelB functional assay. Right-side-out (RSO) membrane vesicles containing $MelB_{St}$ or $MelB_{Ec}$ were treated with DDM or GNG-3,14. Following ultracentrifugation, the resulting MelB extracts were subjected to the binding assay with melibiose reversal of FRET from Trp to dansyl-2-galactoside (D^2G). Changes in fluorescence emission intensity were monitored over the course of a sequential addition of D^2G and an excess amount of melibiose at the 1-min and 2-min time points, respectively (red line, DDM; orange line, GNG-3,14). Addition of water instead of excess melibiose at the 2-min time point was the control (pale brown line).

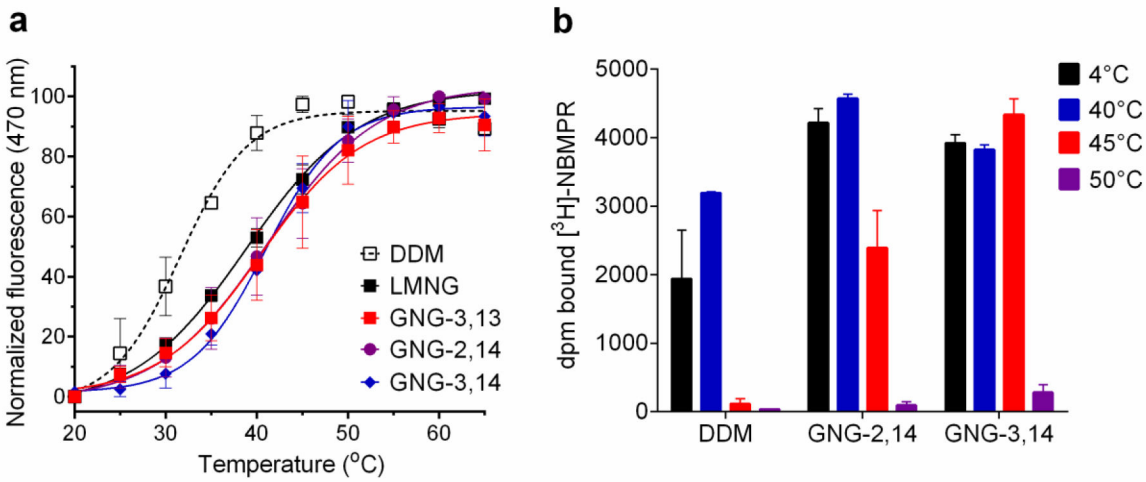

Figure 5.

Thermostability of MOR (a) and hENT1 (b) dissolved in DDM, LMNG or a selected P-GNG (GNG-2,14, GNG-3,13 and GNG-3,14). For MOR study, DDM-purified receptor was added to buffer solutions containing the individual detergents to allow detergent exchange. For hENT1 study, the transporter was extracted and solubilized from the membrane using 1.0 wt% each detergent and the resulting samples were subjected to centrifugation. T_m of MOR was estimated via CPM assay at a detergent concentration of 0.5 wt%. Detergent exchange was omitted for DDM sample due to protein instability in this detergent. hENT1 stability was assessed by measuring the ligand binding ability of the transporter using the radioactive ligand ([^{3}H]-nitrobenzylmercaptopurine ribonucleoside (NBMPR)) after a 30-min incubation at four different temperatures (4, 40, 45, or 50 °C). Error bars, SEM; n = 2-3 (MOR) or n = 2 (hENT1).

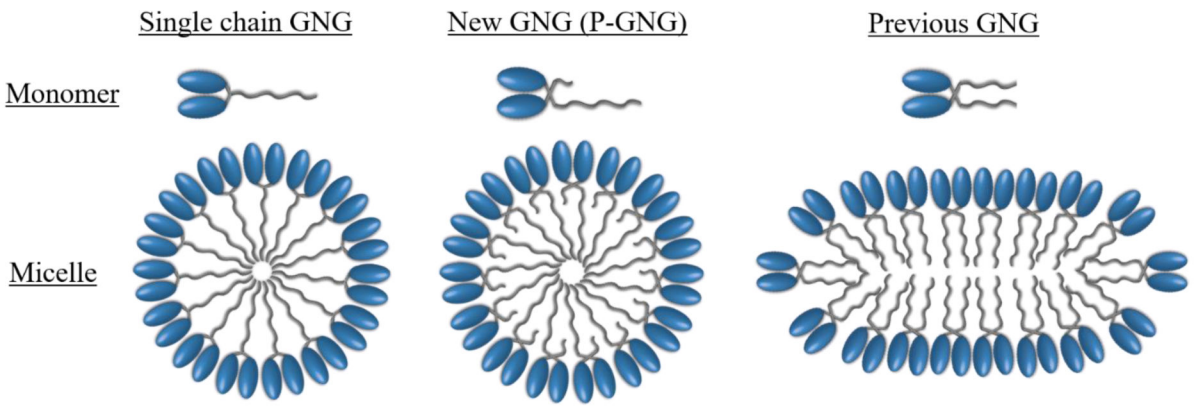

Figure 6.

Illustration of detergent micelles formed by a hypothetical single chain GNG, the newly prepared P-GNG and the previously reported GNG. The pendant group of the P-GNG is well accommodated in the empty spaces existing within micelles formed by single chain GNG and thus plays a favorable role in strengthening the hydrophobic interactions between detergent molecules. The previously developed GNG forms micelles with two alkyl chains of the same length and thus likely contains relatively large empty spaces in the hydrophilic-hydrophobic interfaces.

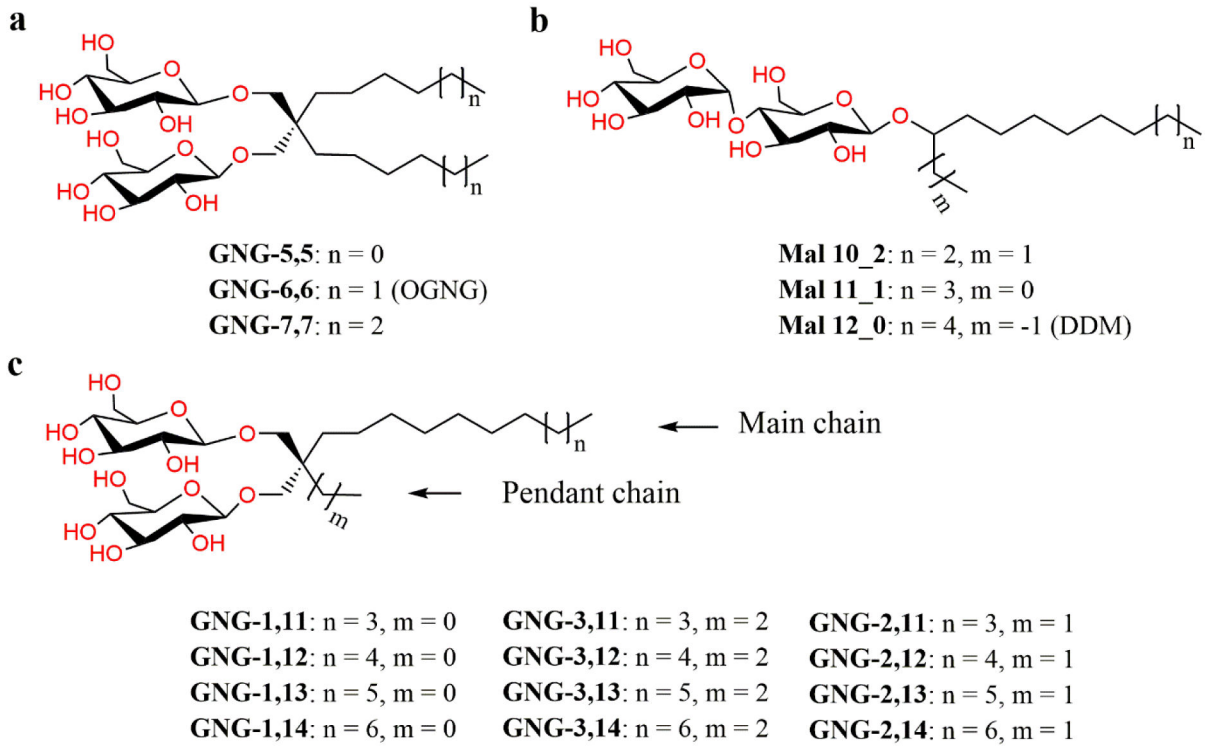

GNG-5,5: n = 0
GNG-6,6: n = 1 (OGNG)
GNG-7,7: n = 2

Mal 10_2: n = 2, m = 1
Mal 11_1: n = 3, m = 0
Mal 12_0: n = 4, m = -1 (DDM)

GNG-1,11: n = 3, m = 0	**GNG-3,11**: n = 3, m = 2	**GNG-2,11**: n = 3, m = 1
GNG-1,12: n = 4, m = 0	**GNG-3,12**: n = 4, m = 2	**GNG-2,12**: n = 4, m = 1
GNG-1,13: n = 5, m = 0	**GNG-3,13**: n = 5, m = 2	**GNG-2,13**: n = 5, m = 1
GNG-1,14: n = 6, m = 0	**GNG-3,14**: n = 6, m = 2	**GNG-2,14**: n = 6, m = 1

Scheme 1.

Chemical structures of previously reported GNGs (a) and branch-chained maltosides (b), and newly prepared pendant-bearing GNGs (P-GNGs) (c). All the GNG agents share a branched diglucoside hydrophilic group (a,c), but while the previous GNGs have two identical alkyl chains (a), the new GNGs contain two different chains (c; main & pendant chain) in a lipophilic region. The chain length of the main alkyl group varied from C11 to C14, while the pendant chain length varied from C1 (methyl) to C3 (propyl), as indicated by the detergent designation. As for the branch-chained maltosides, the short alkyl pendants of the P-GNGs are present at the interface between the hydrophilic and hydrophobic groups. GNG-6,6 and Mal 12_0 correspond to conventional detergents of OGNG and DDM, respectively.

Table 1.

Molecular weights (*MW*s), critical micelle concentrations (CMCs; mean ± SD, $n = 3$) of P-GNGs, OGNG and DDM and hydrodynamic radii (R_h; mean ± SD, $n = 5$) of their micelles in water at room temperature.

Detergent	*MW*[a]	CMC (μM)	R_h (nm)[b]
GNG-1,11	568.7	190 ± 15	2.82 ± 0.02
GNG-1,12	582.7	100 ± 8	2.93 ± 0.03
GNG-1,13	596.8	38 ± 2	3.08 ± 0.10
GNG-1,14	610.8	26 ± 1	3.26 ± 0.01
GNG-2,11	582.7	150 ± 1	2.76 ± 0.02
GNG-2,12	596.8	70 ± 2	3.04 ± 0.03
GNG-2,13	610.8	30 ± 2	3.19 ± 0.06
GNG-2,14	624.8	24 ± 1	3.20 ± 0.03
GNG-3,11	596.8	100 ± 3	2.77 ± 0.01
GNG-3,12	610.8	38 ± 3	2.89 ± 0.03
GNG-3,13	624.8	22 ± 3	3.05 ± 0.09
GNG-3,14	638.8	23 ± 2	3.22 ± 0.03
OGNG	568.7	~1000	4.46 ± 0.15
DDM	510.6	170	3.47 ± 0.04

[a] Molecular weight of detergents.

[b] Hydrodynamic radius of detergents measured at 1.0 wt% by dynamic light scattering.